Boundary-Layer Meteorol (2007) 122:263–272
DOI 10.1007/s10546-006-9114-0

RESEARCH NOTE

Forward Lagrangian stochastic simulation of a transient source in the atmospheric surface layer

E. H. Shadwick · J. D. Wilson · T. K. Flesch

Received: 3 April 2006 / Accepted: 5 July 2006 /
Published online: 19 October 2006

Abstract We show that a forward Lagrangian stochastic (LS) model simulates well the ensemble-averaged concentration transient due to a short time (5 min) point source in the uniform atmospheric surface layer. In LS models, computational particles, which may not descend below ground level, are necessarily reflected at an imposed (artificial) boundary above ground. Model results were rather insensitive to the placing of the lower reflection boundary, and no definite benefit stemmed from including a parametrization for unresolved delays/displacements beneath the lower boundary.

Keywords Air pollution · Atmospheric dispersion · Lagrangian stochastic model · Transient source · Turbulent trajectories

1 Introduction

The Lagrangian stochastic (LS) model gives arguably the best description of dispersion in a turbulent flow, for it offers conceptual simplicity and flexibility as well as more fundamental advantages, namely of making rational use of all known velocity statistics, and of correctly treating the non-diffusive near field of the source (Wilson and Sawford 1996). There have been numerous demonstrations of the fidelity of LS models with respect to steady-state sources in a stationary atmosphere, where the resulting mean concentration field is independent of the distribution of travel times from source to detector.

Our primary aim in this brief paper is to demonstrate the good performance of even the simplest well-mixed (Thomson 1987) LS model in regard to plume timing, by simulating a simple field experiment with a point source of tracer methane running

E. H. Shadwick (✉) · J. D. Wilson · T. K. Flesch
Department of Earth & Atmospheric Sciences, University of Alberta, 1-26 Earth Sciences Building, Edmonton, AB T6G 3E6, Canada
e-mail: shadwick@ualberta.ca

on a five-minutes-on/five-minutes-off duty cycle. As a secondary aim, since our focus is plume timing, we shall also assess the usefulness of incorporating the formulation of Wilson et al. (2001b) to parameterize the 'surface delays' spent by particles in the unresolved layer beneath the trajectory reflection height z_r, and the corresponding displacements.

2 Transient source experiment

Methane from a gas cylinder was released from a point source at height $h_s = 0.5\,\mathrm{m}$ over short grass, in a horizontally-homogeneous surface layer at the University of Alberta experimental farm, Ellerslie, Alberta (June 22, 2001). The gas flow rate $Q = 20 \pm 21\,\mathrm{min}^{-1}$ was monitored by a rotameter. Nearby, at nominal downwind distances from the source of about 24 and 45 m, two line-averaging infrared lasers monitored methane concentration; their path lengths were respectively 102 and 213 m, and their path height $z_L = 1.5\,\mathrm{m}$.

Two 3-dimensional sonic anemometers (Campbell Scientific CSAT3) at a height of $z_s = 2.12\,\mathrm{m}$ provided meteorological data averaged (during the transient source experiment) over five-minute blocks. During a fortuitous sequence of rather constant (consecutive 5 min) means of wind speed and direction, the source was held on and then off for alternating five-minute cycles. For sonic observations, during the eight "on" periods, indicated that atmospheric stability was effectively neutral; the friction velocity $u_* = 0.43\,\mathrm{m\,s}^{-1}$; the mean "cup" wind speed $S = \overline{\sqrt{u^2 + v^2}} = 3.95\,\mathrm{m\,s}^{-1}$ and mean wind direction 305 deg; and the surface roughness length, which we computed by reconciling the measured friction velocity and mean wind speed according to the usual logarithmic mean wind profile

$$z_0 = z_s \exp\left(-\frac{k_v\, S}{u_*}\right), \tag{1}$$

was $z_0 = 0.054\,\mathrm{m}$, with the von Karman constant $k_v = 0.4$.

The observed concentration time series from the lasers are shown in Figs. 1 and 2. It can be seen that the preceding release does not affect the concentration over the subsequent five-minute release period, i.e. each 'on' period may be regarded as an independent event. Thus the eight 'on' periods recorded during this interval of steady wind speed and direction were used to form an ensemble average against which the simulated concentration trace could be compared. The background methane concentration was deduced (independently for each of the two laser sensors) by averaging the methane concentration over the last four minutes of each 'off' cycle. The resulting concentrations for each of the eight 'off' periods were then ensemble-averaged and taken as a (constant) value for the mean background concentration. The background concentration was adjusted by a retrospective (multiplicative) laser re-calibration so as to present a mean value of 1.9 ppm, which is consistent with the atmospheric concentration of CH_4 listed (by Alberta Environment) for the day the experiment was carried out.[1]

[1] Please note that the concentration time series shown in Figs. 1 and 2 are the *pre-calibration* values.

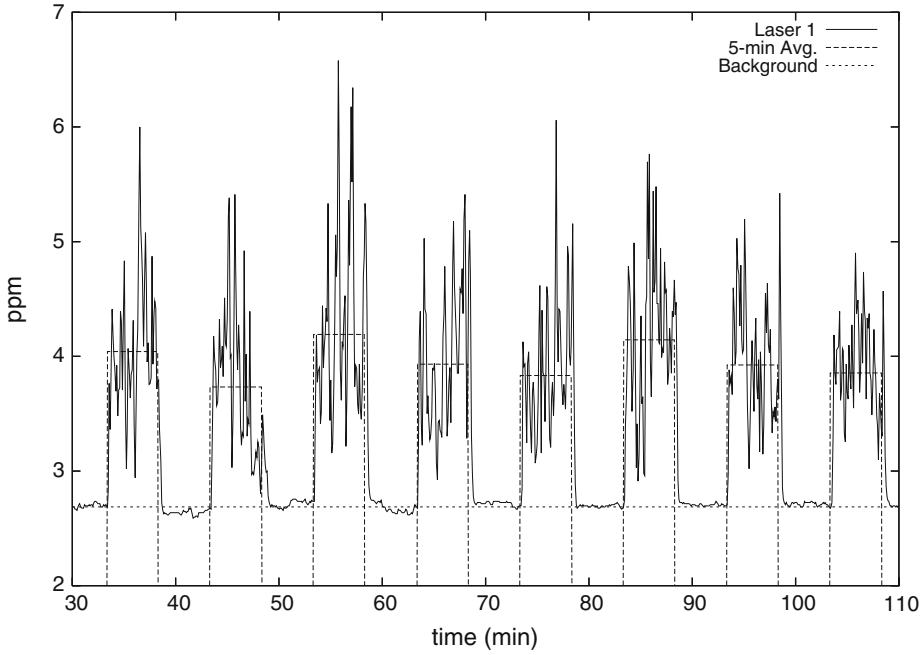

Fig. 1 Concentration time series as recorded by the nearer sensor at a nominal distance of about 24 m from the point source with path length = 102 m. The concentrations shown are the pre-calibration values and have not been scaled to give a background concentration of 1.9 ppm

3 Forward LS model

We adopted an LS model suitable for computing tracer paths in a neutrally-stratified, horizontally-homogeneous surface layer, under the approximation that the velocity probability density functions for the three (Eulerian) velocity fluctuations are independent Gaussians (i.e. we neglect velocity correlations). The unique well-mixed model (Thomson 1987) appropriate to these conditions is

$$du_i = \frac{C_0\,\epsilon\,u_i}{2\sigma_i^2}\,dt + \sqrt{C_0\epsilon}\,d\xi_i, \tag{2}$$

$$dx_i = (u_i + \overline{u}_i)\,dt, \tag{3}$$

(no summation over i in Eq. (2)) where u_i is the Lagrangian velocity fluctuation; $\overline{u}_i = (\overline{u}(z), \overline{v}(z), 0)$ is the mean Eulerian velocity vector; σ_i^2 is the velocity variance along the coordinate direction i; and $d\xi_i$ is a random increment with zero mean and variance dt. We specified the timestep as

$$dt = \mu\,\frac{2}{C_0\epsilon}\,\min\left[\sigma_u^2, \sigma_v^2, \sigma_w^2\right] \tag{4}$$

with $\mu = 0.1$, $C_0 = 3.1$ (consistent with our neglect of velocity correlations: Wilson et al., 2001a), $\sigma_u = \sigma_v = 2u_*$, and $\sigma_w = 1.3u_*$. We parameterized the turbulent kinetic energy dissipation rate by the conventional $\epsilon(z) = u_*^3/(k_v z)$. Equations (2)–(4) were

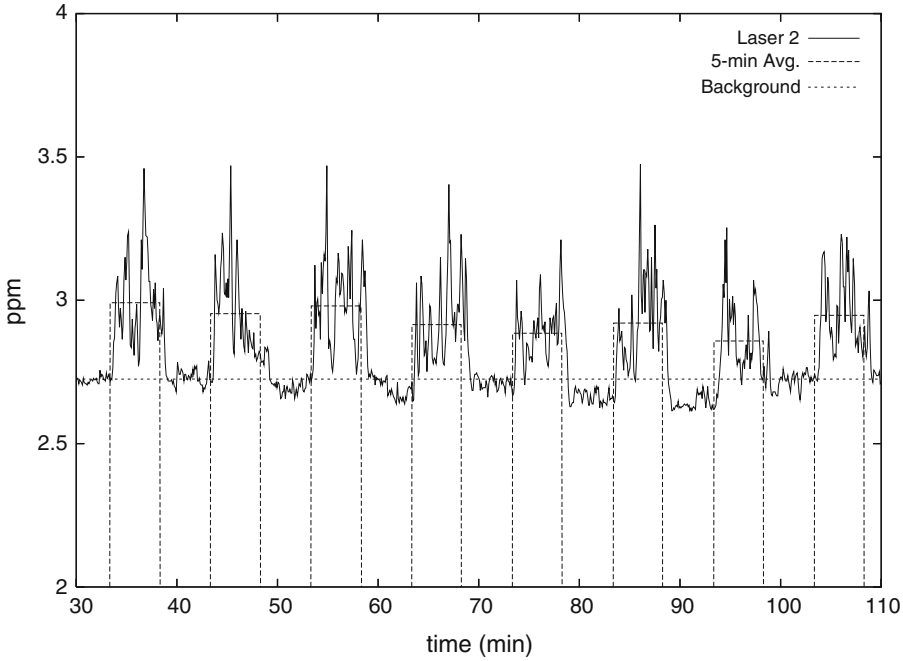

Fig. 2 Concentration time series as recorded by the far sensor, at a nominal distance of about 45 m from the source with path length = 213 m

used to determine an ensemble of trajectories for particles released from a point source.

3.1 Horizontal velocity components of the LS model

As indicated in Fig. 3, we defined the model's y axis as being parallel to the laser path,[2] the mean wind direction β as the deviation-angle away from true north, and β_{mod} the deviation angle away from (the model's) x-axis. Therefore, unless the mean wind ran *perpendicular* to the (chosen) laser path (in which case in our convention the mean wind direction $\beta_{\mathrm{mod}} = 0$ and the mean wind is parallel to the x-axis), it was necessary that both horizontal components of the mean wind should be simulated by the LS model. Following Wilson (2004; Sec. 2g), these components are

$$U(z) = \left(\frac{u_* \cos \beta_{mod}}{k_v}\right) \ln\left(\frac{z}{z_0}\right), \tag{5}$$

$$V(z) = \left(\frac{u_* \sin \beta_{mod}}{k_v}\right) \ln\left(\frac{z}{z_0}\right). \tag{6}$$

As regards the fluctuations in horizontal velocity, due to our approximation of symmetry $\sigma_u = \sigma_v = 2u_*$ we had no need of corresponding rotation formulae for partitioning the velocity variance.

[2] In the experiment the two lasers were not exactly parallel. However the Lagrangian stochastic model was run independently to compute the concentration seen by each laser.

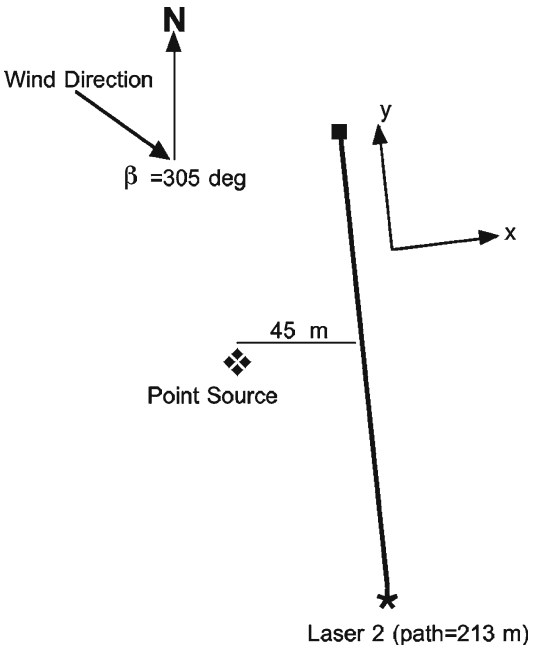

Fig. 3 Set-up of simulation, defining the x, y axes, the orientations of the (selected) laser, and the direction of the mean wind

3.2 Surface reflection

In LS models, particle trajectories are necessarily reflected at an imposed (artificial) boundary z_r (for reflection criteria see Wilson and Flesch 1993; Thomson and Montgomery 1994). The siting of that boundary is to a large extent a matter of convenience, and so one may speed up computations by setting $z_r \gg z_0$, i.e. by reflecting trajectories far above ground, thus obviating the need for calculations in a layer where the high turbulent kinetic energy dissipation rate ϵ necessitates a very small timestep dt. Wilson et al. (2001b) proposed an algorithm to parameterize the surface delays and corresponding spatial displacements experienced by particles descending beneath the lower boundary z_r, and the present work provides an opportunity to assess its utility. The mean delay and mean along wind displacement per reflection proposed by Wilson et al. are

$$\bar{\tau} \approx 2.5 z_r/\sigma_w, \tag{7}$$

$$\bar{\delta} \approx \langle \bar{u}|z_r \rangle \, \bar{\tau}, \tag{8}$$

where $\langle \bar{u}|z_r \rangle$ is the height average of $\bar{u}$ in the layer between z_r and the surface, in the present case

$$\langle \bar{u}|z_r \rangle = \frac{u_* z_0}{k_v (z_r - z_0)} \left[\frac{z_r}{z_0} \ln \left(\frac{z_r}{z_0} \right) - \frac{z_r}{z_0} + 1 \right]. \tag{9}$$

Model trials were run with two choices for the reflection height, $z_r = (z_0, 7z_0)$. The surface-delay algorithm was applied only for trials where $z_r = 7z_0$. The mean displacement per reflection was $\bar{\delta} = 2.31$ m, and the corresponding mean delay was $\bar{\tau} = 1.69$ s. Regarding the anticipated impact of the surface-delay parameterization, it

should be more noticeable in its effect on the fade-away transition at the end of the on-cycle, than in its effect on the onset: this is because, by definition, the trailing edge of the concentration trace at the laser is a contribution from particles that have arrived at the laser tardily, and, therefore, have travelled close to ground. As to whether the correction ought to have a greater impact on modelled concentration at the nearer or farther laser, this is unclear; while the significance of any one reflection (delay 1.69 s) is less significant relative to travel time as the latter increases (i.e. at the downwind laser), the longer travel time causes a proportionate increase in the probable number of reflections preceding arrival.

3.3 Concentration computations

The nearer and farther laser detectors had path lengths respectively of 102 m and 213 m. To model the concentration profile along each laser, its path was divided into 500 equally sized sample volumes with dimensions $\Delta y = (0.204, 0.426)$ m, $\Delta x = \Delta z = 0.3$ m. As we were dealing with a transient source, the model concentration was quantized (and smoothed) not only spatially (index j), but also in time. We set the temporal 'bin' width $\Delta t_b = 5$ s, and we shall index the time axis n. As we set the time origin $t = 0$ to coincide with the source-on transition, each computational particle began its random flight at some time $t \geq 0$.

Whenever a particle traversed a sampling volume the residence time contribution was computed and added to an accumulator for the appropriate location and time window (due to the small dimension of the samplers, traversal normally implied a residency time that was smaller than the timestep Δt). For each sampler the mean residence time $\bar{t}_{j,n}$ (summed and normalised over a large number N_p of independent random flights) in location bin j and time bin n, gives the model's estimate for the mean concentration at that time and place according to

$$C(j\Delta y,\, n\Delta t_b) = \frac{Q\,\bar{t}_{j,n}}{\Delta x\;\Delta y\;\Delta z} \tag{10}$$

where Q (kg s^{-1}) is the (physical) source strength. For the results to be shown, $N_p = 10^5$ particles were released within each time window $\Delta t_b = 5$ s.

4 Discussion

LS model results with trajectory reflection height set to $z_r = (z_0, 7z_0)$ are compared with the observations in Figs. 4 and 5, which show that the model simulates the concentration at both sensor locations quite accurately (see also Table 1). The model concentration trace ramps on at the appropriate time, but wanes slightly early. A shorter time discretisation (i.e. binning width Δt_b) marginally improves the timing at the end of the release period, with the disadvantage of a much noisier estimate of $C(t)$ throughout; using $\Delta t_b = 5$ s represents a reasonable compromise as (for the other given choices, viz. $N_p = 10^5$, etc.) it results in a relatively smooth ensemble-averaged concentration at the two lasers, and furthermore provides a temporal resolution comparable to that provided by the lasers.

LS model results with the application of the surface-delay parameterisation at a reflection height of $z_r = 7z_0$ are shown in Figs. 6–9. Even though the reflection height $z_r = 7z_0 = 0.378$ m was quite close to the height of the source ($h_s = 0.5$ m),

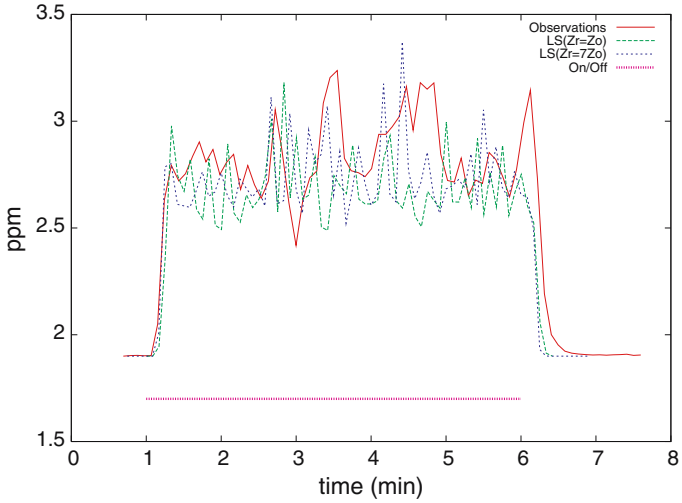

Fig. 4 Comparison of observed trace of (ensemble- and line-averaged) concentration with corresponding prediction of the LS model, for the nearer laser (nominally 24 m from the source, with path length 102 m) with trajectory reflection height $z_r = (z_0, 7z_0)$. The source was turned on $t = 1$ min, and turned off $t = 6$ min

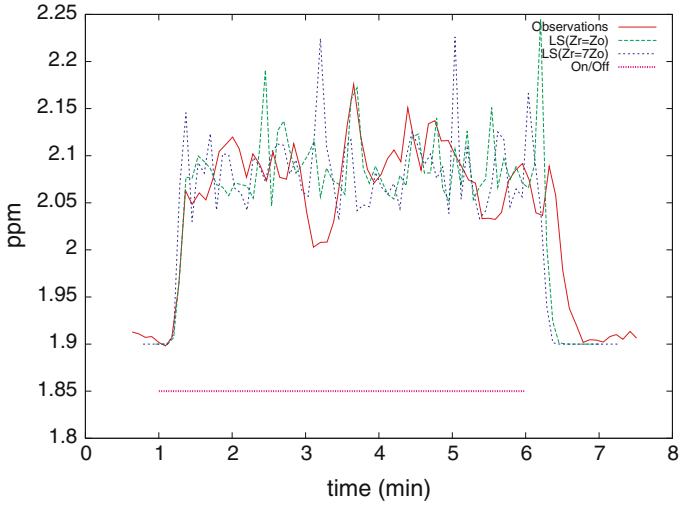

Fig. 5 Comparison of observed trace of (ensemble- and line-averaged) concentration with corresponding prediction of the LS model, for the far laser (nominally 45 m from the source, with path length 213 m) with trajectory reflection height $z_r = (z_0, 7z_0)$

the observed concentrations at both sensor locations are fairly well simulated by the LS model. The (simulated) plume arrival is again slightly premature. This timing is improved with the application of the surface-delay algorithm that matches the off-timing for the case of $z_r = 7z_0$ to that of the case where $z_r = z_0$ for both sensor locations. The improved timing is more easily seen in Figs. 8 and 9 where the LS model and observed concentrations are compared from time $t = 5$ min to time $t = 6$ min.

Table 1 Observed and modelled mean concentrations over the "source on" intervals, for a reflection height of $z_r = z_0$

	Observed	LS
Laser 1	2.80	2.70
Laser 2	2.07	2.08

Concentrations are given in ppm. Laser 1 refers to the near laser, path = 102 m; laser 2 refers to the far laser, path = 213 m

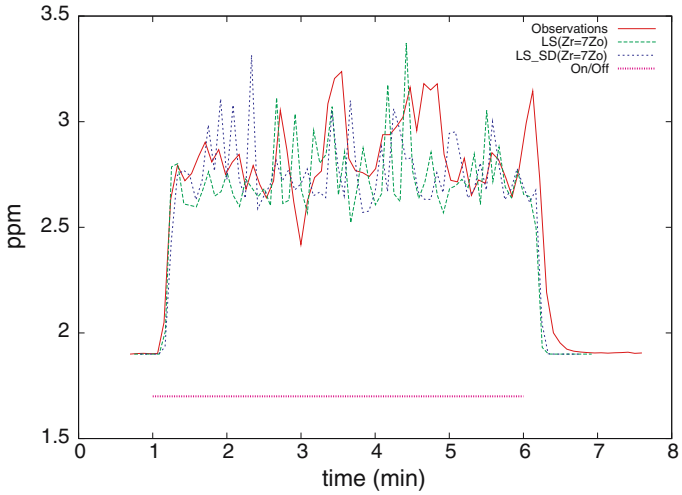

Fig. 6 Comparison of ensemble-averaged observed concentration with LS model concentration for the nearer laser (nominally 24 m from the source, with path length 102 m) with and without the surface-delay algorithm with a reflection height of $z_r = 7z_0$. The label LS_SD refers to the LS model with the application of the surface delay algorithm

For both sensor locations and for both choices of surface-reflection height, the mean concentrations of the LS model are in good agreement with the observed mean concentrations over the 5-min period. Values of mean concentration (with and without the surface-delay parameterization for the case where $z_r = 7z_0$) are summarised in Tables 1 and 2.

From these results it is evident that the impact of the surface delay/ displacement algorithm on the computed concentration transient is small, at least in the case examined (very short range). As expected, the impact was greater at the trailing edge of the concentration transient than at onset. It appears also to be more significant for timing of the concentration transient at the more distant of the two lasers, though this would be a weak basis to generalize that the correction should be more significant for longer range problems. In short, even with a reflection height set not very far beneath the height of the source, there seems to have been negligible penalty for neglecting the mean delay/displacement per reflection.

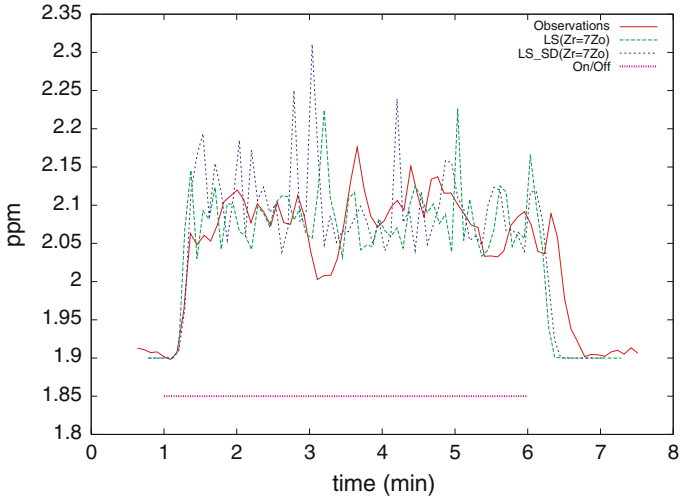

Fig. 7 Comparison of ensemble-averaged observed concentration with LS model concentration for the far laser (nominally 45 m from the source, with path length 213 m) with and without the surface-delay algorithm with a reflection height of $z_r = 7z_0$. The label LS_SD refers to the LS model with the application of the surface-delay algorithm

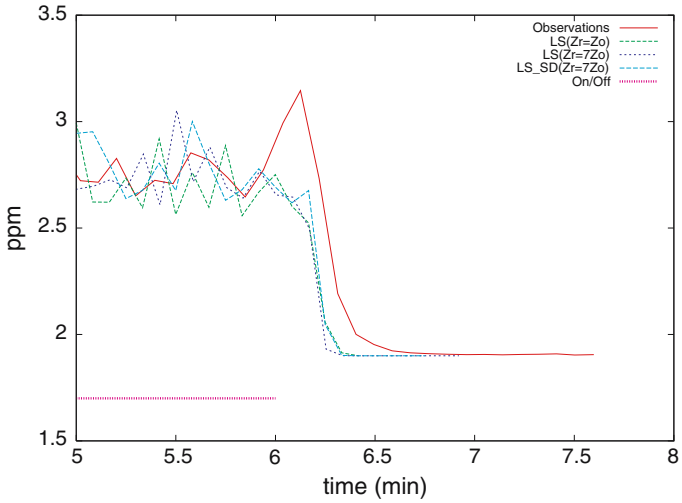

Fig. 8 Comparison of plume fade-off for the nearer laser (nominally 24 m from the source, with path length 102 m) with and without the surface-delay algorithm with reflection height $z_r = (z_0, 7z_0)$

5 Conclusion

By reference to a short-range (order 20–50 m) tracer experiment in a neutral, horizontally-uniform surface layer, we have shown that a simple LS model replicates quite well the (ensemble mean) timing of concentration onset and fade-off due to a transient source, in addition to the mean concentration during on periods. This validation represents another confirmation of the physical plausibility of the Lagrangian stochastic

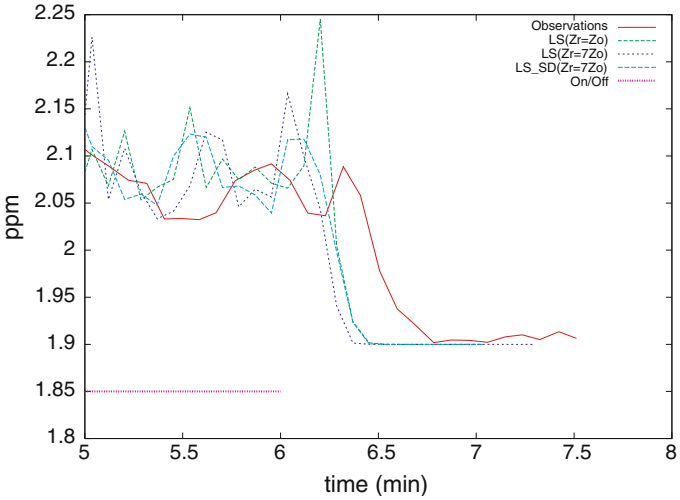

Fig. 9 Comparison of plume fade-off for the far laser (nominally 45 m from the source, with path length 213 m) with and without the surface-delay algorithm with reflection height $z_r = (z_0, 7z_0)$

Table 2 Observed and modelled mean concentrations, with and without the surface-delay algorithm, for a reflection height of $z_r = 7z_0$

	Observed	Delay	No Delay
Laser 1	2.80	2.75	2.70
Laser 2	2.07	2.09	2.08

Concentrations are given in ppm

class of dispersion model. For the case investigated here, the quality of the LS simulations was rather insensitive to the placing (z_r) of the lower reflecting boundary, and there was found to be negligible advantage in incorporating a parameterization for surface delays corresponding to unresolved trajectory segments beneath that height.

Acknowledgements This work has been supported by a research grant from the Natural Sciences and Engineering Research Council of Canada (NSERC).

References

Thomson DJ (1987) Criteria for the selection of stochastic models of particle trajectories in turbulent flows. J Fluid Mech 180:529, 556

Thomson DJ, Montgomery MR (1994) Reflection boundary conditions for random walk models of dispersion in non-gaussian turbulence. Atmos Environ 28:1981–1987

Wilson JD, Flesch TK (1993) Flow boundaries in random flight dispersion models: enforcing the well-mixed condition. J Appl Meteorol 32:1695–1707

Wilson JD, Sawford, BL (1996) Lagrangian stochastic models for trajectories in the turbulent atmosphere. Boundary Layer Meteorol 78:191–210

Wilson JD, Flesch TK, Harper, LA (2001a) Micro-meteorological methods for estimating surface exchange with a disturbed windflow. Agric For Meteorol 107:207–225

Wilson JD, Flesch TK, D'Amours R (2001b) Surface delays for gases dispersing in the atmosphere. J Appl Meteorol 40:1422–1430

Wilson JD (2004) Oblique, stratified winds about a shelter fence, II: comparison of measurements with numerical models. J Appl Meteorol 43:1392–1409